THE ASTROPHYSICAL JOURNAL, 444:244–250, 1995 May 1

CGRO/OSSE OBSERVATIONS OF THE CASSIOPEIA A SUPERNOVA REMNANT

L.-S. THE, M. D. LEISING, AND D. D. CLAYTON
Department of Physics and Astronomy, Clemson University, Clemson, SC 29634-1911
W. N. JOHNSON, R. L. KINZER, J. D. KURFESS, AND M. S. STRICKMAN
E.O. Hulburt Center for Space Research, Naval Research Laboratory, Mail Code 4150, Washington, DC 20375-5320
G. V. JUNG
Universities Space Research Associates, Washington, DC 20375-5320
AND
D. A. GRABELSKY, W. R. PURCELL, AND M. P. ULMER
Department of Physics and Astronomy, Northwestern University, Evanston, IL 60208
Received 1994 August 10; accepted 1994 November 7

ABSTRACT

Cassipeia A, the youngest known supernova remnant in the Galaxy and a strong radio and X-ray source, was observed by OSSE 1992 July 16–August 6. Its close distance (~3 kpc) and its young age (~300 yr) make Cas A the best candidate among known supernova remnants for detecting ^{44}Ti γ-ray lines. We find no evidence of emission at 67.9 keV, 78.4 keV, or 1.157 MeV, the three strongest ^{44}Ti decay lines. From simultaneous fits to the three lines our 99% confidence upper limit to the flux in each line is 5.5×10^{-5} γ cm^{-2} s^{-1}. We also report upper limits for the 4.44 MeV ^{12}C nuclear de-excitation line, which could be produced by interactions of accelerated particles in the supernova remnant, and for the hard X-ray continuum.

Subject headings: gamma rays: observations — ISM: indvidual (Cassiopeia A) — nuclear reactions, nucleosynthesis, abundances — supernova remnants

1. INTRODUCTION

Cassiopeia A (Cas A) is a supernova remnant (SNR) located at $l = 111\overset{\circ}{.}73$, $b = -2\overset{\circ}{.}13$ (Zombeck 1990) near the Galactic plane at a distance of 2.92 kpc (Braun 1985). The radio and optical size of the emission region is 1'.8 (Dickel et al. 1982). The radio emission is nonthermal synchrotron whereas the X-ray emission is thermal in nature. Extrapolating the position of the fast-moving optical knots of the remnant to its center yields an explosion data AD 1658 ± 3 (van den Bergh & Kamper 1983) for a distance of 2.8 kpc (van den Bergh & Dodd 1970). However, Ashworth (1980) claims that John Flamsteed observed the Cas A supernova in 1680 when it was sixth magnitude (Brecher & Wasserman 1980). This generally unnoticed event was so dim that its peak visual magnitude was probably fainter than magnitude 3 (Da Silva 1993; van den Bergh 1991).

Dynamical mass determinations suggest a massive star progenitor. Deceleration can be measured from the difference between the age obtained from extrapolating moving knots to an origin assuming constant velocity (Kamper & van den Bergh 1976) and the age if the explosion was in 1680 (Ashworth 1980). The size, current expansion rate, deceleration, and the particle number density in the ejecta give the mass of ejecta ≥ 10–$12\ M_\odot$ and swept-up mass around 0.8–1.5 $M_\odot$ (Brecher & Wasserman 1980). *Tenma* (Tsunemi et al. 1986) and *EXOSAT* (Jansen et al. 1988) data suggest that the mass of the thermal X-ray–emitting gas is ~2.4 and ~5.8 $M_\odot$, respectively. However, Fabian et al. (1980) used *Einstein Observatory* high-resolution X-ray images of Cas A and the assumption of optically thin thermal emission to estimate the mass of X-ray–emitting gas to be at least 15 $M_\odot$.

Other evidence supports a massive star progenitor for Cas A. Tsunemi et al. (1986) find that the heavy element abundances from X-ray observations roughly agree with those predicted by the Type II supernova model of Woosley & Weaver (1982). There is some evidence that Cas A was a Type Ib supernova (van den Bergh 1991). The supernova spectral evolution might have resembled that of SN 1987K, a SN II–like spectrum near maximum light which emerged as a SN Ib later (Fesen & Becker 1991). WR stars have been suggested to be the progenitors of Type Ib supernovae (Ensman & Woosley 1988). Comparison of surface chemical composition of WR star models with Cas A ejecta suggest that the progenitor was a He- and N-rich WNL star with initial mass between 25 and 60 $M_\odot$ (Fesen & Becker 1991).

Although supernova nucleosynthesis calculations are converging and produce reasonable agreement with cosmic abundances, observing γ-ray lines from radioactive elements in a SNR provides a direct way to investigate the accuracy of the calculations (Clayton, Colgate, & Fishman 1969; Clayton 1974). ^{56}Co (Leising & Share 1990, and references therein) and ^{57}Co (Kurfess et al. 1992) lines from supernova SN 1987A and the ^{26}Al (Mahoney et al. 1984) line from the interstellar medium have been detected and compared to the abundances in supernova models. Attempts to measure other supernova γ-ray lines, such as from radioactive ^{44}Ti, ^{60}Fe, and ^{22}Na from novae, also have been made (Mahoney et al. 1982; Leising et al. 1988; Mahoney et al. 1992; Leising & Share 1994). The proximity of Cas A (~3 kpc) and its young age (~300 yr) make Cas A the best known SNR for detecting ^{44}Ti γ-ray lines. Indeed, that was the primary goal of this OSSE observation. COMPTEL, another *CGRO* experiment, observed Cas A during 1992 July 6–August 6 and 1993 February 25–March 9. Its imaging and spectral analyses show evidence for line emission at 1.16 MeV from the Cas A direction at a significance level of ~4 σ. The line flux derived from COMPTEL data is $(7.0 \pm 1.7) \times 10^{-5} \gamma$ cm^{-2} s^{-1} (Iyudin et al. 1994). Even with the smaller data set described here, OSSE should be able to confirm this detection.

According to nucleosynthesis theory, ^{44}Ti is produced in explosive Si burning, with the largest production in an alpha-rich (low-density) freeze-out of nuclear statistical equilibrium. The requirements for Si burning are shown in Figure 20 of Woosley, Arnett, & Clayton (1973) and Figure 5 of Thielemann, Hashimoto, & Nomoto (1990). In the ejected part of a core collapse supernova, only the incomplete and alpha-rich freeze-out Si-burning processes appear to take place. The normal freeze-out of Si burning operates in Type Ia supernova where the density at freeze-out is higher (Thielemann, Nomoto, & Yokoi 1986). Calculations of ^{44}Ti production (Woosley & Hoffman 1991; Thielemann et al. 1990) show that in order to achieve solar mass fractions of ^{44}Ca, strong alpha-rich freeze-out of Si burning must take place in the objects which produce most of the Galactic iron, probably core-collapse explosions. The ejected amount of ^{44}Ti depends on the mass cut (how much mass falls back onto the neutron star or black hole), the presupernova nuetron excess inside 2 $M_\odot$, and the maximum temperature and density reached during the passage of the shock wave in the ejecta. There are large uncertainties in these quantities, which would be greatly constrained by direct measurements of ^{44}Ti. Typically, both types of supernova models predict ejected ^{44}Ti masses near $10^{-4}\ M_\odot$.

Radioactive ^{44}Ti decays to ^{44}Sc, which emits 67.9 keV (100%) and 78.4 keV (98%) lines, and then decays, with half-life ($t_{1/2}$) 5.7 hr, into ^{44}Ca, which emits a 1.157 MeV (100%) ray line. The half-life ($t_{1/2}$) of radioactive ^{44}Ti is still uncertain, with recent measurements of 46.4 and 66.6 yr (Frekers et al. 1983; Alburger & Harbottle 1990). If M_4 is the mass of ^{44}Ti produced in a supernova in units of $10^{-4}\ M_\odot$, f_γ is the branching ratio of a line per ^{44}Ti decay, $D_{\rm kpc}$ is the distance, and $\tau(=t_{1/2}/\ln 2)$ is the decay lifetime, the line flux at Earth is

$$F_\gamma = F_0\, f_\gamma\, M_4\, \frac{\exp\,(-t/\tau)}{D_{\rm kpc}^2}\ \gamma\ {\rm cm}^{-2}\ {\rm s}^{-1}\,, \qquad (1)$$

where $F_0 = 0.72/\tau$ (yr) cm^{-2} s^{-1} is the initial flux (unattenuated) from $10^{-4}\ M_\odot$ of ^{44}Ti at $D_{\rm kpc} = 1$. F_0 ranges from 7.50×10^{-3} to 10.8×10^{-3} as the ^{44}Ti half-life ranges from 66.6 to 46.4 yr.

Galactic ^{44}Ti γ-ray lines have been sought by the γ-ray spectroscopy experiments on *HEAO* 3 (Mahoney et al. 1992) and the *SMM* satellite (Leising & Share 1994). Mahoney et al. (1992) obtain a 99% confidence level for 67.9 and 78.4 keV line fluxes of $2 \times 10^{-4}\gamma$ cm^{-2} s^{-1}. Leising & Share (1994) searching the 10 yr data of *SMM* for the 1.16 MeV line from ^{44}Sc $\rightarrow$ ^{44}Ca decay place an upper limit of $8 \times 10^{-5}\gamma$ cm^{-2} s^{-1} from the general direction of the Galactic center at 99% confidence. Their analysis of the upper limits constrains the Galactic supernova rate and the amount of ^{44}Ti produced in supernovae. For example, Leising & Share (1994) find that the modest supernova rate of 1.5 century^{-1} is consistent with their 1.16 MeV ^{44}Ti line measurements at only 5% confidence. Higher rates are less probable. Combining the record of six Galactic supernova in the last millenium and the upper limits on the ^{44}Ti γ-ray line flux yields further constraints (Hartmann et al. 1993, 1993).

It is widely believed that supernova ejecta/interstellar medium shocks accelerate energetic particles. The energetic particles within the SNR not only produce Kα X-rays, but can also excite nuclear levels which then decay by photon emission (Meneguzzi & Reeves 1975). Bussard, Ramaty, & Omidvar (1978) found that the 4.44 MeV ^{12}C line should be the strongest line produced. They used the upper limit to the broad iron line flux at 6.8 keV to constrain the broad and narrow components of the 4.44 MeV ^{12}C line to 2.8×10^{-4} and $2.7 \times 10^{-5}\gamma$ cm^{-2} s^{-1}, respectively. As these fluxes are possibly detectable with OSSE, we also search our data for these features.

The X-ray continuum up to 30 keV and X-ray lines from Cas A have been detected by many investigators. X-rays from SNRs are thermal in nature and are generated by the interaction of the ejecta with the interstellar medium (McKee 1974; Gull 1975; Itoh 1977; Hamilton, Sarazin, & Chevalier 1983). Pravdo & Smith (1979) measured a temperature of 10^8 K for the 5–25 keV range using *HEAO* A-2. They interpreted the continuum as arising from optically thin plasma in the collisionless shock fronts. Two isothermal plasmas with temperatures of 0.65 and 4 keV were needed to fit the *Einstein Observatory* data (Becker et al. 1979, 1980), supporting the idea of a shock-heating model in which the cooler temperature is due to a reverse shock in the ejecta and the higher temperature is due to circumstellar material shocked by the primary blast wave. However, the X-ray spectra of *Tenma* (2–12 keV) did not require a two-component model and could be fitted with single thermal bremsstrahlung continuum with temperature of 4.4×10^7 K, if several emission features from intermediate mass elements are included in a nonequilibrium ionization model (Tsunemi et al. 1986). Observations over a wider energy range of 0.5–25 keV by *EXOSAT* (Jansen et al. 1988) found that the X-ray continuum can be fitted with a model with two temperatures of 3.3×10^7 and 7.5×10^6 K, with a non-ionization equilibrium condition required. Another recent interpretation of the X-ray spectrum suggests that the power-law form of the hard X-ray spectrum is due to the bremsstrahlung from accelerated electrons at shock fronts (Asvarov et al. 1989). The energy spectrum of electrons accelerated in the shock by the regular mechanism (Bell 1978) has the same form as the electrons producing the synchrotron emission in the radio range. Asvarov et al. (1989) use this electron spectrum to calculate the bremsstrahlung emission in the hard ($\geq$30 keV) X-ray spectrum. The spectrum shown in their Figure 1 is very near the OSSE hard X-ray sensitivity.

2. OBSERVATIONS AND DATA ANALYSIS

The OSSE observation of Cas A was performed during the *Compton Observatory* viewing period 34, 1992 days 198–219. The total observing time was 3×10^5 s. The OSSE spectral analysis technique subtracts background measured in offset pointings of the detectors from the source pointing (Johnson et al. 1993). Figure 1 shows the field of the Cas A observation, including the source and the two background pointings, in Galactic coordinates. The size of the emission region in radio and optical wavelengths of Cas A is 1.8 (Dickel et al. 1982), well inside the field of view of OSSE. The quadratically interpolated background estimates are subtracted from the source spectrum to obtain a difference spectrum for each 2 minute integration. Detailed description and performance of the OSSE instrument can be found elsewhere (Johnson et al. 1993). The average of all spectra from four detectors over the entire observing period is shown in Figure 2. It is this spectrum we search for evidence of ^{44}Ti line emission.

3. ^{44}Ti γ-RAY LINES

To extract line fluxes we fit the count spectra with various continuum photon spectra plus one or more Gaussians at the

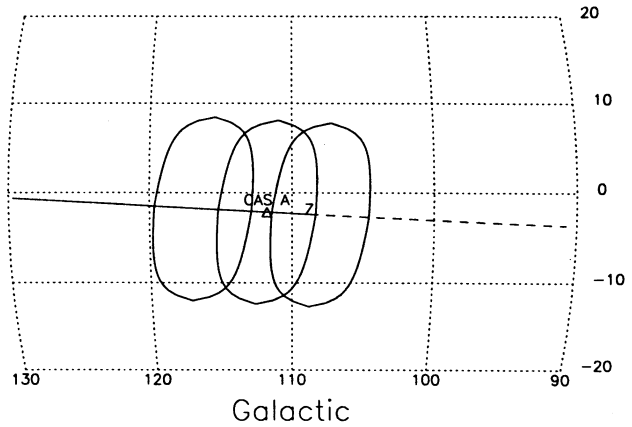

FIG. 1.—Field of view of OSSE Cas A observation. The source and background fields are shown in Galactic coordinates. The contours show the OSSE 10% response level. The OSSE scan range is shown as a solid line. The character *Z* near Cas A shows the *Z*-axis pointing of the *CGRO* spacecraft.

energies of interest. These photon spectra are folded through the four detector OSSE instrument responses, and the resulting four count models are least-squares fitted to the respective four detector energy-loss spectra. In no case do we find significant continuum emission. Since Cas A is currently expanding at $\leq 10{,}000$ km s^{-1}, we fix the intrinsic line widths to 2.5% of line rest energies.

Fit results are tabulated in Table 1 and shown in Figure 3. Figure 3*a* shows the average count spectra of four OSSE detectors over energy range of 0.04–0.11 MeV with fit models overlaid. A best fit of two Gaussian features 67.9 and 78.4 keV and an exponential photon continuum for the range 0.04–0.11 MeV is shown in Figure 3*a* as a dashed line. The OSSE cannot resolve these two lines, so they would appear as a single broad peak. In all fits we fix the ratio of the 68 keV line flux to the 78 keV line flux to 0.98. Of course, the actual signature of ^{44}Ti is three lines. The solid line shows the result of fitting the count spectra from 0.04 to 0.11 MeV with an exponential continuum and from 0.8 to 1.4 MeV with a linear continuum, and the three strongest ^{44}Ti lines *simultaneously*. The ratio of the 1.157 MeV line flux to that of the 68 keV line is fixed at unity. A fit of an exponential continuum without lines is shown as a dotted line, which almost coincides with the fit with three lines (solid line). For illustration we also show as a dashed-dotted line the expected OSSE count rate with all three line fluxes fixed at the COMPTEL flux of $7.0 \times 10^{-5}\gamma$ cm^{-2} s^{-1}. Figure 3*b* shows the average count spectra of four OSSE detectors in the energy range 1.05–1.25 MeV. Also shown are the fitted models consisting of continuum only (dotted line), a single Gaussian line at 1.157 MeV only (dashed line), and all three ^{44}Ti lines (best-fit: solid line; fluxes fixed at $7.0 \times 10^{-5}\gamma$ cm^{-2} s^{-1}: dash-dot line).

We find no evidence for ^{44}Ti line emission. The best fit of only the 68 and 78 keV lines with an exponential continuum between 0.04 and 0.11 MeV gives each flux of $(+3.23 \pm {}^{2.33}_{2.54}) \times 10^{-5}\gamma$ cm^{-2} s^{-1}. The best fit of the 1.157 MeV line alone with a 0.8–1.4 MeV linear continuum is $(-5.62 \pm 4.03) \times 10^{-5}\gamma$ cm^{-2} s^{-1}. The best fit to three lines plus separate continua in the ranges 0.04–0.11 and 0.8–1.4 MeV linear continuum is $(+0.40 \pm {}^{2.26}_{2.77}) \times 10^{-5}\gamma$ cm^{-2} s^{-1} for each line. We have also included the 511 keV line from annihilation of $^{44}\text{Sc} \rightarrow {}^{44}\text{Ca}$ positrons (95%) in one model by fixing the flux ratio of the 511 keV line to that of the 68 keV line to a value of 0.95. The best simultaneous four-line fit gives a flux for the 68 keV line of $(-0.61 \pm 1.70) \times 10^{-5}\gamma$ cm^{-2} s^{-1}. A fit of a 511 keV Gaussian line alone gives a line flux of $(-0.54 \pm {}^{3.35}_{3.05}) \times 10^{-5}\gamma$ cm^{-2} s^{-1}. However, since the lifetime of positrons in a SNR is uncertain, we report the final results here using the fit from the 68 keV, 78 keV, and 1.157 MeV lines. The various continuum models are used only to assess the effects of the continuum choice on the measured line fluxes. We see no significant continuum emission, and the line results change very little even if no continuum component is included in the models. We use the three line fit to establish an upper limit to ^{44}Ti emission from Cas A. This is derived by measuring the increase of the minimum χ^2 versus the line flux in fits with fixed line fluxes but with all other parameters allowed to vary freely. The 99% confidence upper limit to the flux of each of the three ^{44}Ti γ-ray lines is $5.1 \times 10^{-5}\gamma$ cm^{-2} s^{-1}. Considering statistical uncertainties only, the OSSE and COMPTEL measurements are formally consistent with each other at 1.8% confidence, for a true flux value of $4.7 \times 10^{-5}\gamma$ cm^{-2} s^{-1}.

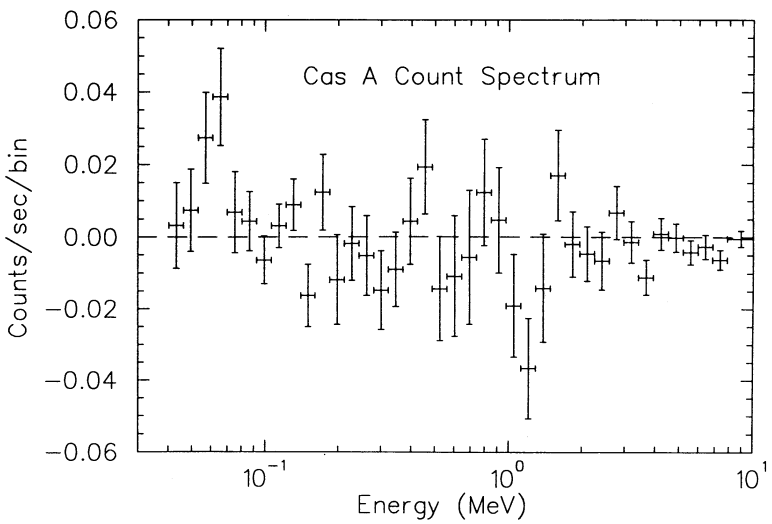

FIG. 2.—Average OSSE count spectra of Cas A from 22 day observation with four detectors

TABLE 1

MEASURED Cas A LINE FLUXES

Source	Energy (keV)	Continuum (MeV)	Flux[a]	χ^2_ν	D.O.F.	99% Upper Limit[a]
^{44}Ti.....	67.9 and 78.4[b]	Exponential (0.04–0.11)	$(+3.23 \pm {}^{2.33}_{2.54})$	1.64	44	8.6
	1157	Linear (0.80–1.40)	(-5.62 ± 4.03)	0.98	390	3.8
	67.9, 78.4, and 1157[c]	Exponential and Linear (0.04–0.11 and 0.80–1.40)	$(+0.40 \pm {}^{2.26}_{2.77})$	1.03	443	5.1
	67.9, 78.4, 511.0, and 1157[d]	Exponential(0.04–1.40)	(-0.61 ± 1.70)	1.05	905	3.4
	511.0	Exponential (0.3–0.7)	$(-0.54 \pm {}^{3.35}_{3.05})$	1.02	267	6.0
^{12}C	4.438 narrow	Linear (3.00–6.00)	(-1.74 ± 2.74)[e]	...	...	4.6
	4.438 broad	Linear (3.00–6.00)	$(+6.14 \pm 5.13)$[f]	0.87	296	18.0

[a] Flux in each line in units of $10^{-5}\gamma\ \mathrm{cm}^{-2}\ \mathrm{s}^{-1}$.
[b] Simultaneous fit to 68 keV and 78 keV lines.
[c] Setting the 68 keV, 78 keV, and 1.157 MeV line fluxes to ratios of 1:0.98:1.
[d] Setting the 68 keV, 78 keV, 511 keV, and 1.157 MeV line fluxes to ratios of 1:98:0.95:1.
[e] Simultaneous fit to the narrow (FWHM = 0.050 MeV) and the broad (FWHM = 0.50 MeV) components of the 4.438 MeV line of ^{12}C to the 3.0–6.0 MeV count spectra. This is the narrow component flux.
[f] Same as noted, but for the broad component.

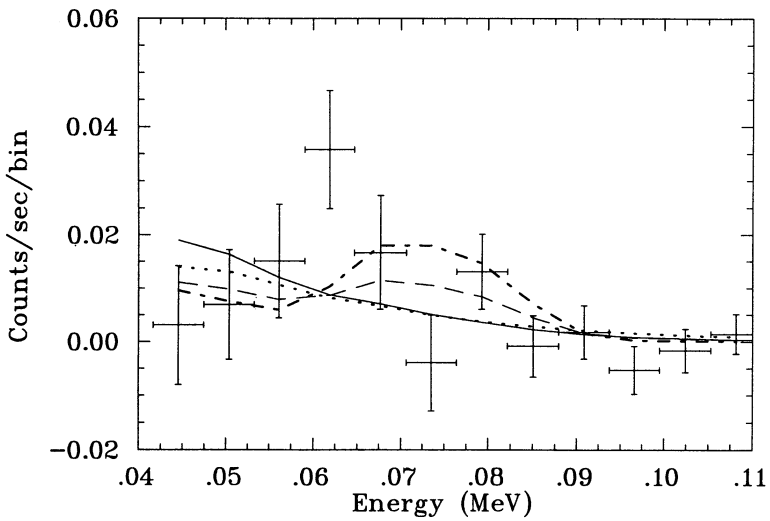

FIG. 3*a*

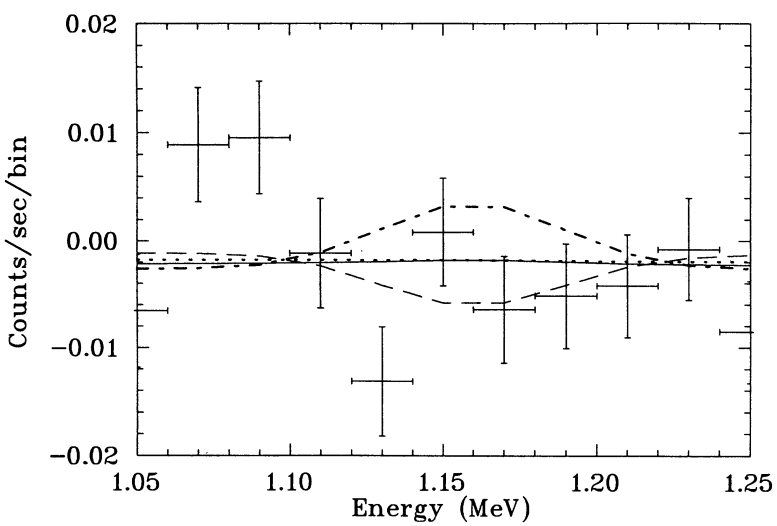

FIG. 3*b*

FIG. 3.—(*a*) Average count spectrum from 0.04 to 0.11 MeV with fitted models overlaid. The solid line is the best simultaneous fit to the separate ranges 0.04–0.11 MeV and 0.8–1.4 MeV with independent continua and three ^{44}Ti decay γ-ray lines with fixed flux ratios of 1:0.98:1. The best-fit line amplitude $(+0.40 \pm {}^{2.26}_{2.77}) \times 10^{-5}\gamma\ \mathrm{cm}^{-2}\ \mathrm{s}^{-1}$ is too small to be seen. The dashed-dotted line is the same fit with the line fluxes fixed at a value of $7.0 \times 10^{-5}\gamma\ \mathrm{cm}^{-2}\ \mathrm{s}^{-1}$ (see Iyudin et al. 1994). The dashed line is the best fit to the energy range of 0.04–0.11 MeV *only* with an exponential continuum and the 68 keV and the 78 keV lines fitted simultaneously. The dotted line is a fit of an exponential continuum only. (*b*) Same as (*a*) but for energy range 1.05–1.25 MeV. Note that the spectrum in this range of energy has been rebinned for presentation in the figure, however, the fits were done with the native bins of the four OSSE detectors (see Table 1 for parameters).

To search for possible systematic effects in the OSSE data and analysis system, especially in view of the formally negative flux at 1.157 MeV, we analyzed similarly the spectra of 139 separate OSSE observations of active galaxies (Johnson et al. 1994). We expect no ^{44}Ti emission from those fields and we find no evidence for any. The measured line fluxes are generally consistent with the null hypothesis. However, fitting the 1.157 MeV line alone gives a mean flux of $(-1.1 \pm 0.5) \times 10^{-5}\gamma$ cm^{-2} s^{-1}, with the individual measurements approximately normally distributed about that value. To allow for a possible systematic error at this level we add $0.4 \times 10^{-5}\gamma$ cm^{-2} s^{-1} to our three-line upper limit (1.157 MeV line is one of the three ^{44}Ti lines in the fit), making it $5.5 \times 10^{-5}\gamma$ cm^{-2} s^{-1}.

4. ^{12}C γ-RAY LINES

We also fit the 4.44 MeV ^{12}C γ-ray lines with both 50 keV and 500 keV Gaussian widths simultaneously between 3.0 and 6.0 MeV. We find no evidence of either feature. We show in Table 1 the 99% upper limits of 4.6×10^{-5} and $1.8 \times 10^{-4}\gamma$ cm^{-2} s^{-1}, respectively.

5. γ-RAY CONTINUUM

We find no evidence for continuum emission from Cas A. We show in Figure 4 the X-ray spectra from *HEAO* A-2 (Pravdo & Smith 1979), *Tenma* (Tsunemi et al. 1986), and *EXOSAT* (Jansen et al. 1988) together with OSSE upper limits. We also superpose the accelerated electron bremsstrahlung model of Asvarov et al. (1989). The OSSE data are consistent with the extrapolation of the X-ray spectra. A power-law fit to *HEAO* A-2 data yield a power-law index of $\sim$3.41. Fitting this power law to OSSE data below 200 keV gives χ^2/dof = 1.63 with dof (degree of freedom) = 5, and fitting both *HEAO* A-2 and OSSE data below 200 keV yields a power-law index of $\sim$2.7.

We have no significant detection of continuum emission. Formally, the Cas A continuum in the energy range 0.04–0.11 MeV is best fitted by an exponential continuum, $(6.41 \pm 4.10) \times 10^{-3}$ exp $[(E-0.05\ \text{MeV})/kT]\gamma$ cm^{-2} s^{-1} MeV^{-1} with $kT = (1.87 \pm 1.20) \times 10^{-2}$ MeV, $\chi^2_\nu = 1.64$, and dof = 45. When we fit the same energy range with a power-law continuum ($dn/dE \propto E^{-\gamma}$), we find the power-law index $\gamma = (3.37 \pm 2.34)$. We do not expect the thermal bremsstrahlung process that produces X-rays below 20 keV detected by *HEAO* A-2, *Einstein Observatory*, *Tenma*, and *EXOSAT* to produce emission detectable by OSSE at $E \geq 50$ keV. For example, the two-temperature plasma model used to fit the *EXOSAT* spectra (Jansen et al. 1988) predicts a flux of only $4.9 \times 10^{-6}\gamma$ cm^{-2} s^{-1} MeV^{-1} at 50 keV. However, a model proposed by Asvarov et al. (1989) predicts a detectable flux from Cas A. Hard X-rays are produced by the bremsstrahlung from shock-accelerated electrons, which are also responsible for the synchrotron emission in the radio with spectral index, $\alpha = 0.76$ where $S_\nu \propto \nu^{-\alpha}$ (Baars et al. 1977; Allakhverdiyev et al. 1986; Anderson et al. 1991). Asvarov et al. (1989) derive the hard X-ray flux

$$F_\gamma(E) = 3.83 \times 10^{-4} f n_i Z^2 K_X C(\alpha) \times \frac{D_{\rm pc}^3}{d_{\rm kpc}^2} E^{-(\alpha+1.5)}\gamma \text{ cm}^{-2} \text{ s}^{-1} \text{ keV}^{-1}, \quad (2)$$

where n_i is the density of ions with the charge Z, K_X is the normalization factor of accelerated electron density related to synchrotron emission in radio range, $C(\alpha)$ is the constants tabulated in Asvarov et al. (1989), $D_{\rm pc}$ is the diameter of the SNR in pc, $d_{\rm kpc}$ is the distance to the SNR, and f is the volume filling factor (=0.25 in Sedov model).

The dashed line in Figure 4 (with $\gamma = 2.26$) is drawn following equation (2) using the parameters given in Asvarov et al. (1989). The fit of this spectrum to OSSE data below 200 keV gives a χ^2/dof = 1.43 with dof = 111. More sensitive observations are needed to show if there actually is hard X-ray emission above 30 keV as proposed by Asvarov et al. (1989).

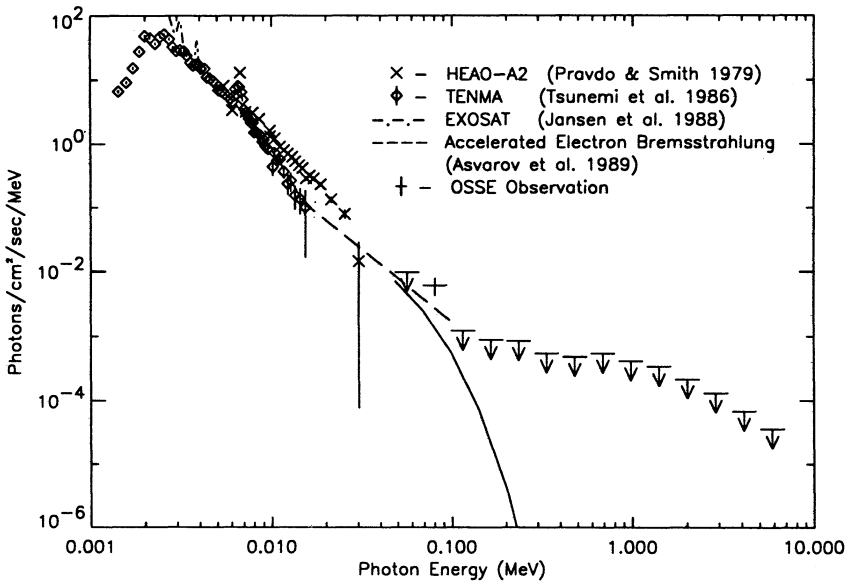

FIG. 4.—Cas A broad-band photon spectrum. This figure shows that the continuum upper limits from OSSE measurements are consistent with the extrapolation of X-ray thermal bremsstrahlung data from *HEAO* A-2, *Tenma*, and *EXOSAT* and also with the accelerated electron bremsstrahlung for energy above 16 keV (see text). OSSE upper limits are 2 σ. The solid line is an exponential fit to the energy range 0.04–1.4 MeV.

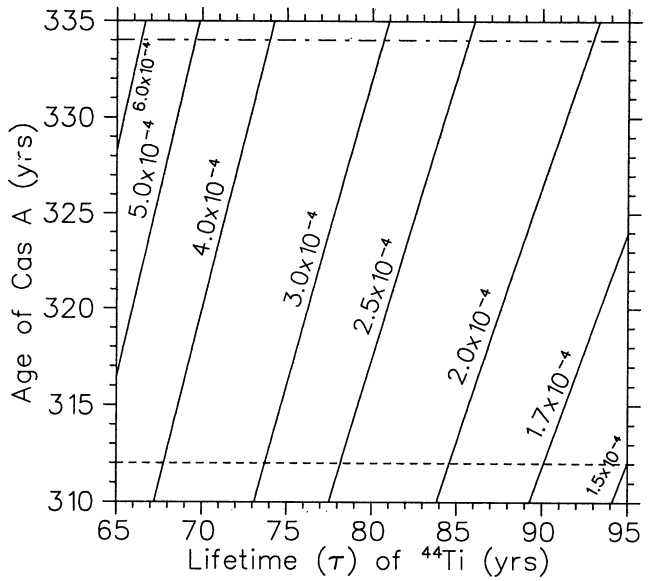

FIG. 5.—Plot of the amount of ^{44}Ti in Cas A in units of $M_\odot$ as a function of ^{44}Ti mean lifetime (τ) and the age of Cas A. The ^{44}Ti mass is calculated using eq. (1) with distance to Cas A of 2.92 kpc and ^{44}Ti line flux of $5 \times 10^{-5} \gamma$ cm^{-2} s^{-1}. The dashed line shows the age of Cas A from Flamsteed's observation (Ashworth 1980). The dashed-dotted line is the age of Cas A from extrapolating the position of the fast-moving optical knots of Cas A to a center of explosion (van den Bergh & Dodd 1970).

6. DISCUSSION

The relation between the ^{44}Ti line flux from Cas A and the amount of ^{44}Ti is uncertain due to the uncertainties in the date of the explosion, the ^{44}Ti lifetime, and the distance to Cas A. The distance is between 2.8 and 3.0 kpc, which causes only about 15% uncertainty in the amount of ^{44}Ti. In Figure 5 we take the distance equal to 2.92 kpc (Braun 1985) and show the range of ^{44}Ti masses at explosion allowed by the age and lifetime uncertainties, for the flux $5 \times 10^{-5} \gamma$ cm^{-2} s^{-1}. This value is chosen because it is roughly the OSSE upper limit and is also nearly the most probable value to resolve the OSSE/COMPTEL discrepancy. This figure shows that the lifetime of ^{44}Ti gives the largest uncertainties. The ^{44}Ti mass values to the lower right of Figure 5 are consistent with the ^{44}Ti mass ($\sim 1 \times 10^{-4}\ M_\odot$) produced in supernova models of Type Ia, Ib, or II (Woosley & Hoffman 1991; Thielemann et al. 1990; Hashimoto et al. 1989; Ensman & Woosley 1988; Nomoto, Thielemann, & Yokoi 1984; Woosley & Weaver 1982).

The COMPTEL experimenters report 1.157 MeV flux from Cas A near $7 \times 10^{-5} \gamma$ cm^{-2} s^{-1} at 4 σ statistical significance (Iyudin et al. 1994). The two measurements are formally consistent at less than 2.0% confidence. If systematic errors can be safely ignored in both OSSE and COMPTEL analyses, the true value of the ejected ^{44}Ti mass is very nearly as displayed in Figure 5. This suggests a somewhat larger value than in typical supernova models, and if correct, also argues for a longer value for the ^{44}Ti lifetime.

The amount of ^{56}Ni produced in a supernova determines its brightness and can be estimated roughly from the amount of ^{44}Ti, if it is known. The COMPTEL 1.157 MeV flux of $7.0 \times 10^{-5} \gamma$ cm^{-2} s^{-1} would imply that the amount of ^{44}Ti at the time of explosion was *at least* $1.9 \times 10^{-4}\ M_\odot$ (obtained with the closest distance, 2.8 kpc, longest ^{44}Ti lifetime, 96.1 yr, and most recent explosion date 1680). Even this minimum amount of ^{44}Ti is on the high side of ^{44}Ti production in supernova nucleosynthesis calculations. Recent models of a core-collapse supernovae with piston-generated explosions and with progenitor masses between 12 and 35 $M_\odot$ (Woosley & Weaver 1994) show that the ratio of mass fractions $X(^{56}\text{Ni})/X(^{44}\text{Ti})$ is $\gtrsim 530$ (this minimum value is for a 12 $M_\odot$ progenitor; Hoffman et al. 1994) while the solar ratio is 812. Therefore the expected amount of ^{56}Ni is $\gtrsim 0.10\ M_\odot$. A supernova with this amount of ^{56}Ni would have a peak visual magnitude of roughly -4 at 3 kpc, assuming no interstellar absorption. The Cas A supernova should have been quite a bright object for several weeks, as a supernova drops only ~ 2 mag in V from its peak in two to three weeks. Thus, as pointed out by Hoffman et al. (1994), the large amount of ^{44}Ti implied by the COMPTEL observation heightens the puzzle of why the high-declination Cas A supernova event was recorded only at magnitude 6 (Ashworth 1980).

The OSSE cannot confirm the COMPTEL detection of ^{44}Ti decay lines. Clearly more observations of Cas A by both instruments are demanded to settle this important question.

We find no evidence of ^{12}C de-excitation lines at flux levels near those calculated for Cas A. We also searched for ^{56}Fe* and ^{26}Mg* γ-ray lines and 511 keV electron-positron annihilation radiation, and we find no evidence of emission in any of these lines. The larger than 50 keV continuum limits are just consistent with the extrapolation of nonthermal bremsstrahlung models from lower energies (Asvarov et al. 1989). Further observations are required to discriminate among models which explain the less than 25 keV emission.

We thank D. McCammon for generously providing us with his compilation of the photoelectric absorption cross sections and D. Bhattacharya, L. Brown, and D. Hartmann for very useful discussions. This research was supported by NASA DPR S-10987C.

REFERENCES

Alburger, D. E., & Harbottle, G. 1990, Phys. Rev. C, 41, 2320
Allakhverdiyev, A. O., Asvarov, A. I., Guseinov, O. H., & Kasumov, F. K. 1986, Ap&SS, 123, 237
Anderson, M., Rudnick, L., Leppik, P., Perley, R., & Braun, R. 1991, ApJ, 373, 146
Ashworth, W. B. 1980, J. History Astron., 11, 1
Asvarov, A. I., Guseinov, O. Kh., Dogel, V. A., & Kasumov, F. K. 1989, Soviet Astron. 33, 532
Baars, J. W. M., Genzel, R., Pauliny-Toth, I. I. K., & Witzel, A. 1977, A&A, 61, 99
Becker, R. H., Holt, S. S., Smith, B. W., White, N. E., Boldt, E. A., Mushotzky, R. F., & Serlemitsos, P. J. 1979, ApJ, 234, L73
———. 1980, ApJ, 235, L5
Bell, A. R. 1978, MNRAS, 182, 147
Braun, R. 1985, Ph.D. thesis, Leiden State Univ.
Brecher, K., & Wasserman, I. 1980, ApJ, 240, L105
Bussard, R. W., Ramaty, R., & Omidvar, K. 1978, ApJ, 220, 353
Clayton, D. D. 1974, ApJ, 188, 155
Clayton, D. D., Colgate, S. A., & Fishman, G. 1969, ApJ, 155, 75
DaSilva, L. A. L. 1993, Ap&SS, 202, 215
Dickel, J. R., Murray, S. S., Morris, J., & Wells, D. C. 1982, ApJ, 257, 145
Ensman, L., & Woosley, S. E. 1988, ApJ, 333, 754
Fabian, A. C., Willingale, R., Pye, J. P., Murray, S. S., & Fabbiano, G. 1980, MNRAS, 193, 175
Fesen, R. A., & Becker, R. H. 1991, ApJ, 371, 621
Frekers, D., et al. 1983, Phys. Rev. C, 28, 1756
Gull, S. F. 1975, MNRAS, 171, 263
Hamilton, A. J. S., Sarazin, C. L., & Chevalier, R. A. 1983, ApJS, 51, 115
Hartmann, D., The, L.-S., Clayton, D. D., Leising, M., Mathews, G., & Woosley, S. E. 1993, A&AS, 97, 219

Hartmann, D., The, L.-S., Clayton, D. D., Leising, M. D., Mathews, G., & Woosley, S. E. 1992, in Proc. Compton Observatory Science Workshop, ed. C. R. Shrader, N. Gehrels, & B. Dennis (NASA CP-3137), 388
Hashimoto, M., Nomoto, K., & Shigeyama, T. 1989, A&A, 210, L5
Hoffman, R. D., et al. 1994, preprint
Itoh, H. 1977, PASJ, 29, 813
Iyudin, A., et al. 1994, A&A, 284, L1
Jansen, F., Smith, A., Bleeker, J. A. M., De Korte, P. A. J., Peacock, A., & White, N. E. 1988, ApJ, 331, 949
Johnson, W. N., et al. 1993, ApJS, 86, 693
———. 1994, in The Second Compton Symposium, ed. C. E. Fichtel et al. (New York: AIP), 515
Kamper, K. W., & van den Bergh, S. 1976, ApJS, 32, 351
Kurfess, J. D., et al. 1992, ApJ, 399, L137
Leising, M. D., & Share, G. H. 1990, ApJ, 357, 638
———. 1994, ApJ, 424, 200
Leising, M. D., Share, G. H., Chupp, E. L., & Kanbach, G. 1988, ApJ, 328, 755
Mahoney, W. A., Ling, J. C., Jacobson, A. S., & Lingenfelter, R. E. 1982, ApJ, 262, 742
Mahoney, W. A., Ling, J. C., Wheaton, W. A., & Higdon, J. C. 1992, ApJ, 387, 314
Mahoney, W. A., Ling, J. C., Wheaton, W. A., & Jacobson, A. S. 1984, ApJ, 286, 578
McKee, C. F. 1974, ApJ, 188, 335
Meneguzzi, M., & Reeves, H. 1975, A&A, 40, 91
Nomoto, K., Thielemann, F. K., & Yokoi, K. 1984, ApJ, 286, 644
Pravdo, S. H., & Smith, B. W. 1979, ApJ, 234, L195
Thielemann, F.-K., Hashimoto, M.-A., & Nomoto, K. 1990, ApJ, 349, 222
Thielemann, F.-K., Nomoto, K., & Yokoi, K. 1986, A&A, 158, 17
Tsunemi, H., Yamashita, K., Masai, K., Hayakawa, S., & Koyama, K. 1986, ApJ, 306, 248
van den Bergh, S. 1991, Phys. Lett., 204, 385
van den Bergh, S., & Dodd, W. W. 1970, ApJ, 162, 485
van den Bergh, S., & Kamper, K. W. 1983, ApJ, 268, 129
Woosley, S. E., Arnett, W. D., & Clayton, D. D. 1973, ApJS, 26, 231
Woosley, S. E., & Hoffman, R. D. 1991, ApJ, 368, L31
Woosley, S. E., & Weaver, T. A. 1982, in Essays in Nuclear Astrophysics, ed. C. A. Barnes, D. D. Clayton, & D. N. Schramm (Cambridge: Cambridge Univ. Press), 377
———. 1994, in preparation
Zombeck, M. V. 1990, Handbook of Space Astronomy and Astrophysics (Cambridge: Cambridge Univ. Press), 64